Structure Design and Ansys Simulation of New Electromagnetic Wave Resistivity Logging Instrument While Drilling

Xiaoqiu Li

School of Mechanical Engineering, Qilu University of Technology (Shandong Academy of Sciences), Jinan 250353, China

*Ll1035401833@163.com

Abstract

Azimuth electromagnetic wave resistivity instruments entered a new era characterized by enhanced quality, elevated standards, and heightened requirements. The purpose of measurement is evolving from conventional resistivity imaging to the detection of formation interfaces and the identification of formation anisotropy. Alongside advancements in electronic circuit architecture, significant improvements have also been made in the mechanical structure. Building upon the main antenna design, both the mechanical architecture are realized, with particular focus on the structural design of the electronic circuit bin and instrument body. At the end, Ansys simulation was used to test the stability and reliability of the mechanical structure, leading to the development of a novel azimuth electromagnetic wave resistivity logging instrument.

Keywords

Logging While Drilling; Mechanical Design; Azimuth Resistivity Log.

1. Introduction

Oil, natural gas, and other resources play a crucial strategic role for every nation and serve as the lifeblood of national industries. Domestic oil service giants are focusing on enhancing scientific and technological research while the introduction of electromagnetic wave LWD technology in the 1980s, the utilization of electromagnetic wave resistivity logging instruments has witnessed vigorous growth due to their ability to predict reservoir interfaces in advance, adjust drilling direction accordingly, and facilitate efficient exploration of oil and gas reserves.

2. Structure Design of New Resistivity While Drilling Instrument

Considering factors such as stability, reliability, integration theory design, electronic circuit planning, and maintenance, the mechanical structure design of the new electromagnetic wave resistivity logging into two main modules: the antenna module and the electronic circuit bin module. The antenna module consists of various types of instrument antenna structures while the electronic circuit module installs required electronic components with power supply, communication, control functions.
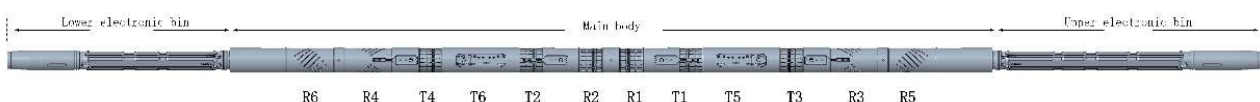

Figure 1. Overall structure of the instrument

The azimuth-while-drilling resistivity instrument, as depicted in Figure 1.1, consists of a main component and an electronic bin module. The main component comprises a six-sending and six-receiving antenna configuration1, T2, T3, and T4 represent vertically oriented Z-direction transmitting antennas. Additionally, T5 and T6 denote horizontally aligned X-direction symmetric transmitting antennas R1 and R2 correspond to vertically oriented Z-direction receiving antennas; R3 and R4 signify coplanar tilt 45° receiving antennas; finally, R5 and R6 indicate receiving antennas tilted at 45° on different planes.

The Z-direction antenna is primarily responsible for transmitting and receiving electromagnetic waves along the instrument's axis (Z direction). It is situated on the side wall of the instrument and comprises an antenna ring slot and 18 ferrite cutting slots. To generate a more efficient magnetic field, the ferrite slot has a width of 5mm and depth of 14mm. The cutting slots are orthogonal to the antenna ring slot and point towards the main axis. A sealed connector hole is designed at the far end of the slot body from the magnetic core, where a three-core sealed connector is placed wiring purposes. The shape of the magnetic core slot is curved with rounded corners measuring 1mm on both sides at its bottom, facilitating placement and sealing.

For the design of X antenna, a symmetrical structure is employed to achieve optimal electromagnetic field distribution and space efficiency, while ensuring interchangeability. The antenna is parallel to the axis of the instrument structure with a fixed magnetic material positioned between them, providing additional protection through an outermost redesigned shell. The dimensions of the X antenna are 250mm in length, 64mm in width, and an average depth of 13mm. Considering structural strength and electronic warehouse connection requirements, a slight reduction of 1mm in depth is necessary; whereas for the storage antenna section, an increase of 1mm in depth is needed to accommodate winding thickness. A total of 11 bolts are used for complete fastening with each bolt hole designed with an interior hole for bolt preload removal.

The 45° inclined antenna can be classified into two types: coplanar and heteroplane. Coplanar refers to an antenna with a 45° angle relative to the Z-axis of the XZ plane instrument, while heteroplane means that a 45° angle with the YZ plane. Although these two structures are similar magnetic field orientation. There are a total of 17 ferrite slots in which 8 slots are symmetrically one is aligned along the axis of the instrument. Each ferrite slot is evenly distributed, and its midpoint connects to an ellipse at a 45° angle to the Z-axis. The length and, allowing for placement of identical ferrite cores. The assembly process for the inclined 45° antenna is identical to that for the Z-axis antenna, thereby enhancing interchangeability and reusability.

The upper/lower electronic bin features a drill collar outer wall embedded structure, which is divided into two silos - upper and lower. These silos primarily accommodate the motherboard, launching board, receiving board, tuning board, and other components. The upper/lower electronic circuit bin is positioned adjacent to the main section on the left (right) side to facilitate power supply and information exchange. On the right (left, it interfaces with external connections for seamless transfer of measurements or rotary steering equipment.

3. Combined Simulation of Weight on Bit and Torque of the Main Body

This simulation is an experiment in static simulation. The primary material selection includes non-magnetic stainless steel P550 or Inconel718. non-magnetic stainless steel P550 as an example, it is a high nitrogen chromium manganese non stainless steel widely utilized in various fields such as ships, aerospace, and petroleum instruments. Through high temperature annealing and gas soft oxidation processes, its surface hardness, wear resistance, and temperature resistance are significantly improved to enhance the material's service life. On the other hand, structural steel generally does not undergo heat treatment due to its relatively simple production process. The yield limit of structural steel is approximately 235MPa while that of non-magnetic stainless steel P550 reaches 965MPa; thus there exists a substantial performance gap between the two materials. Therefore, in this statics experiment, we consider the obtained results for structural steel reasonable enough to infer it instead of non-

magnetic stainless steel P550 is also justifiable. Considering differences in actual performance between domestic and imported materials along with lower material properties of structural steel compared to those of non-magnetic stainless steel P550 and Inconel718; if the simulated results for structural steel are deemed reasonable, it implies that employing non-magnetic stainless steel P550 and Inconel718 as primary drill collar materials is also rationalized accordingly. Henceforth, replacing these materials with structural steels within the simulation experiment.
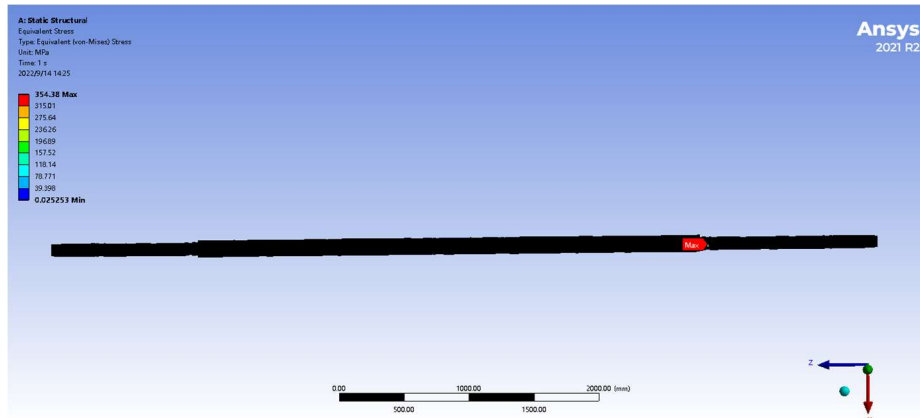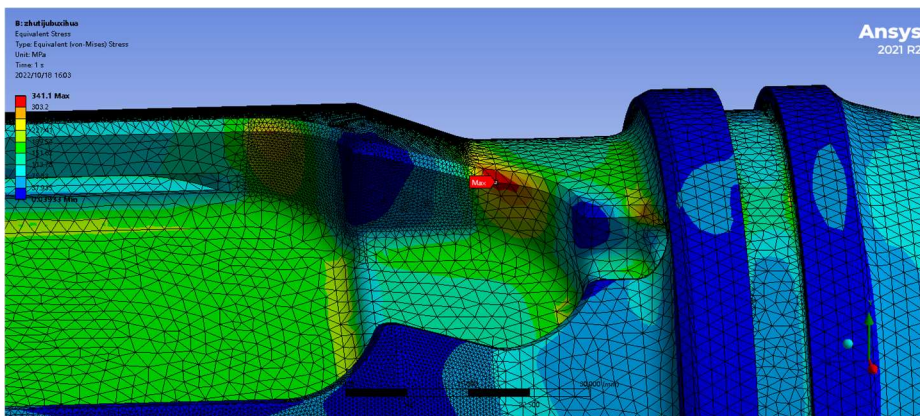

Figure 2. Simulation results

Figure 3. Position of maximum stress

The maximum stress and strain are observed to be concentrated at the sudden diameter change (from a large diameter to a small diameter), as depicted in Figure -3.2. It is worth noting that these irregular and uneven sections, which primarily occur at the diameter change, may introduce potential errors in the simulation result of 341.1MPa. Therefore, it is essential to validate this outcome through secondary simulations.

Considering the concentration of maximum stress and strain at the instrument's diameter reduction, it is imperative to redistribute more in these areas, refine the grid division, and a smaller finite element. Based on the reducer's processor computation capacity, and memory capacity, a 0.5mm mesh was redivided as illustrated in Figure 3.3 below.

After the mesh refinement, the stress at the reducing diameter of the electronic circuit bin decreases from 341.1 MPa to 340.05 MPa, indicating that the observed stress concentration phenomenon is a genuine simulation result and not attributable to human error. Considering both weight on bit and torque simulations, the pressure exerted on the main body remains below 170 MPa, while local stress at the diameter reduction of the electronic circuit bin measures 340.5 MPa. The simulated results for weight on bit and torque applied to the instrument's main within a reasonable range.
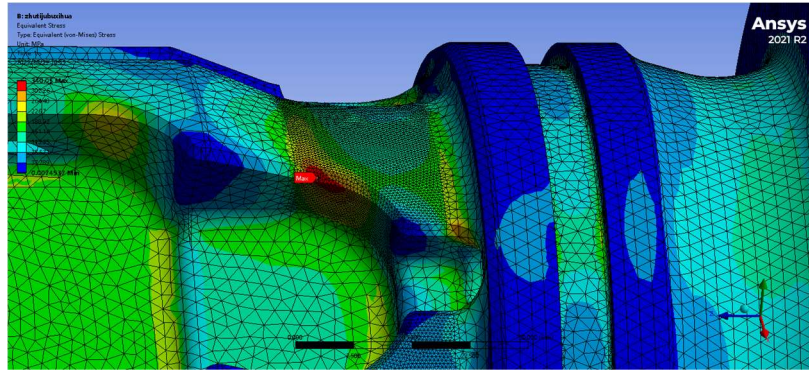
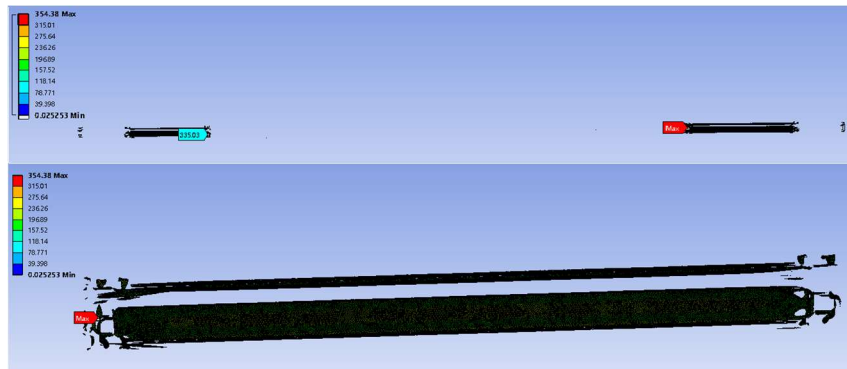**Figure 4.** Mesh refinement of maximum stress position

Figure 5. Cover contour below 170Mpa

4. Conclusion

This paper presents the electronic planning design and mechanical structure realization, with the main antenna of azimuth resistivity instrument used as the anchor point. The completion of the electronic circuit bin structure and's primary mechanical structure is followed by the design of a three-dimensional holographic azimuth electromagnetic wave resistivity model.

In order to assess the structural reliability of the 3D model, Ansys software is employed for conducting structural function simulations that replicate real downhole conditions, with particular emphasis on critical structural components. The simulation results are then utilized to progressively refine and enhance the 3D model.

References

[1] Bittar M . Applying ultra-deep LWD resistivity technology successfully in a SAGD operation[J]. World Oil, 2019(5):240.

[2] Z.M.Wang, H.L.Wang, et al. Mechanical and electrical interface standardization of drilling instruments promotes product industrialization [J]. Technical Supervision of Petroleum Industry,2017,33(12):19-22.

[3] J.Z. Ma, Research and application of Double shoulder drill collar in logging while drilling [J]. China Petroleum and Chemical Industry Standards and Quality,2021,41(09):133-134.

[4] Y.L. Tao, The present situation and development trend of intelligent drilling technology to explore [J]. Journal of petrochemical construction, 2022, 44 (02) : 151-153. The DOI: 10.16264 / j.carol carroll nki. 1672-9323.2022.02.032.